JPET Fast Forward. Published on February 6, 2023 as DOI: 10.1124/jpet.122.001362
This article has not been copyedited and formatted. The final version may differ from this version.

Structural analogs of the GABAkine (5-(8-ethynyl-6-(pyridin-2-yl)-4H-benzo[*f*]imidazole[1,5-α][1,4]diazepin-3-yl) oxazole) (KRM-II-81) are orally bioavailable anticonvulsants without sedation[1]

Kamal P. Pandey[1#], Branka Divović[2#], Farjana Rashid[1#], Lalit K. Golani[1#], Rok Cerne[3,4,5], Nicolas M. Zahn[1], Michelle Jean Meyer[1], Leggy A. Arnold[1], Dishary Sharmin[1], Md Yeunus Mian[1], Jodi L. Smith[3], Xingjie Ping[4], Xiaoming Jin[4], Arnold Lippa[6], V. V. N. Phani Babu Tiruveedhula[1], James M. Cook[1,6], Miroslav M. Savić[2], and Jeffrey M. Witkin[1,3,6]

[1]Department of Chemistry & Biochemistry

University of Wisconsin-Milwaukee, Milwaukee, WI, USA

[2]Department of Pharmacology, Faculty of Pharmacy, University of Belgrade, Belgrade, Serbia

[3]Laboratory of Antiepileptic Drug Discovery

St. Vincent's Hospital, Indianapolis, IN USA

[4]Department of Anatomy and Cell Biology

Indiana University/Purdue University, Indianapolis, IN, USA

[5]Faculty of Medicine, University of Ljubljana, Zaloška cesta 4, Ljubljana, Slovenia.

[6]RespireRx Pharmaceuticals Inc, Glen Rock, NJ, USA

# These authors contributed equally to the manuscript

JPET Fast Forward. Published on February 6, 2023 as DOI: 10.1124/jpet.122.001362
This article has not been copyedited and formatted. The final version may differ from this version.

Running Title Page

Running Title: KRM-II-81 Analogs

Correspondence:

Kamal P. Pandey

kppandey@uwm.edu

or

Jeff Witkin

witkinconsult@gmail.com

Non-standard Abbreviations

AUC: area under the curve

CryoEM: cryogenic electron microscope

EEG: electroencephalogram

FR-II-60: 5-(6-(2-chlorophenyl)-8-ethynyl-4*H*-benzo[f]imidazo[1,5-α][1,4]diazepin-3-yl)oxazole

GABAAR – $GABA_A$ receptor

hERG – human Ether a-go-go related gene = KCNH2

KPP-III-34: 2-(8-bromo-6-(pyridin-2-yl)-4*H*-benzo[f]imidazo[1,5- α][1,4]diazepin-3-yl)-4-ethyloxazole

KPP-III-51: 4-ethyl-2-(8-ethynyl-6-(pyridin-2-yl)-4*H*-benzo[f]imidazo[1,5- α] [1,4]diazepin-3-yl)oxazole

KRM-II-81 - (5-(8-ethynyl-6-(pyridin-2-yl)-4H-benzo[*f*]imidazole[1,5-α][1,4]diazepin-3-yl) oxazole)

PBR: peripheral benzodiazepine receptor

PK: pharmacokinetic

PTZ: pentylenetetrazol

Document Statistics

Tables	9
Figures	9
Pages	32
Abstract	245 words
Introduction	564 words
Discussion	1399 words

JPET Fast Forward. Published on February 6, 2023 as DOI: 10.1124/jpet.122.001362
This article has not been copyedited and formatted. The final version may differ from this version.

Abstract

In order to provide back-up compounds to support the development of the $GABA_A$ receptor (GABAAR) potentiator, KRM-II-81, three novel analogs were designed: replacement of the pyridinyl with Cl-phenyl (FR-II-60), changing the positions of the N and O atoms in the oxazole ring with addition of an ethyl group (KPP-III-34 and KPP-III-51), or substitution of a Br atom for the ethynyl of KRM-II-81 (KPP-III-34). The compounds bound to brain GABAARs. Intraperitoneal administration of FR-II-60 and KPP-III-34 produced anticonvulsant activity in mice (maximal electroshock (MES)-induced seizures or 6 Hz-induced seizures) whereas KPP-III-51 did not. Although all compounds were orally bioavailable, structural changes reduced the plasma and brain (FR-II-60 and KPP-III-51) exposure relative to KRM-II-81. Oral administration of each compound produced dose-dependent increases in the latency for both clonic and tonic seizures and the lethality induced by pentylenetetrazol (PTZ) in mice. Since KPP-III-34 produced the highest brain AUC exposures, it was selected for further profiling. Oral administration of KPP-III-34 suppressed seizures in corneal-kindled mice, hippocampal paroxysmal discharges in mesial temporal lobe epileptic mice, and PTZ-induced convulsions in rats. Only transient sensorimotor impairment was observed in mice and doses of KPP-III-34 up to 500 mg/kg did not produce impairment in rats. Molecular docking studies demonstrated that all compounds displayed a reduced propensity for binding to α1His102 compared to the sedating compound alprazolam; the bromine-

substituted KPP-III-34 achieved the least interaction. Overall, these findings document the oral bioavailability and anticonvulsant efficacy of three novel analogs of KRM-II-81 with reduced sedative effects.

Significance Statement

Sedation and tolerance development are obstacles to the development of improved antiepileptic drugs. A new non-sedating compound, KRM-II-81, with reduced propensity for tolerance is currently moving into clinical development. All three compounds were orally bioavailable, produced anticonvulsant effects in rodents, and displayed low cytotoxicity and sensorimotor impairment. An advanced compound, KPP-III-34, demonstrated efficacy in models of pharmacoresistant epilepsy. Molecular docking studies demonstrated a low propensity for compound binding to the α1His102 residue implicated in sedation. Thus, three additional structures have thus been added to the list of non-sedating imidazodiazepine anticonvulsants that could serve as backups in the clinical development of KRM-II-81.

JPET Fast Forward. Published on February 6, 2023 as DOI: 10.1124/jpet.122.001362
This article has not been copyedited and formatted. The final version may differ from this version.

Introduction

Potentiators of $GABA_A$ receptors (GABAARs) or GABAkines have tremendous value in the therapeutics of neurological (e.g., epilepsy) and psychiatric (e.g., anxiety) disorders. For example, diazepam (Valium®) is on the World Health Organization's List of Essential Medicines. However, GABAkines can come with a risk of tolerance development, abuse, and dependence liability, along with sedative and motor-impairing effects (see Cerne et al., 2021). The search for GABAkines without these safety and side-effect issues has been ongoing in earnest since the discovery of receptor subtypes (Klepner et al., 1979; Lippa et al., 1982, 1981, 1978). The recent U.S. FDA approval of brexanolone (Zulresso®) has led to a resurgence of new GABAkines entering clinical development (Cerne et al., 2021; Witkin et al., 2022). As recently as March 2022, another GABAkine (ganaxolone or Ztalmy®) was approved for seizure control in patients with CDKL5 deficiency disorder (FDA-CDER, 2022).

An imidazodiazepine GABAkine, KRM-II-81 (Witkin et al., 2022), is currently being readied for IND-enabling safety studies. In rodent models, KRM-II-81 has demonstrated anxiolytic-like efficacy (Poe et al., 2016; Witkin et al., 2017), antidepressant-like activity (Methuku et al., 2018), anticonvulsant activity (Knutson et al., 2020; Witkin et al., 2020, 2018), and efficacy in a host of acute and chronic pain models in rodents (Cerne et al., 2022). The efficacy of KRM-II-81 is coupled with an intriguing side-effect profile that includes low sedative and motor-impairing effects, along with a lack of tolerance

development, and abuse liability (Cerne et al., 2021; Witkin et al., 2022). KRM-II-81 is active in models predicting efficacy in pharmacoresistant epilepsy (Witkin et al., 2020). In cortical slices from patients with pharmacoresistant epilepsy, KRM-II-81 has demonstrated suppression of hyperactivity across the neuronal network (Witkin et al., 2018). As an anticonvulsant, KRM-II-81 does not develop tolerance (Witkin et al., 2020). In a murine model of neuropathic pain, no analgesic tolerance was observed (Biggerstaff et al., 2020). In the intracranial self-stimulation model that detects drugs of abuse, KRM-II-81 did not show activity (Moerke et al., 2019). And, when studied as a discriminative stimulus, another model used to predict abuse liability, KRM-II-81 did not fully reproduce the effects of midazolam (Lewter, 2019).

Given the pharmacological profile of KRM-II-81, chemistry in the imidazodiazepine structural series has continued (e.g., (Knutson et al., 2020; Pandey et al., 2020). In the present manuscript, the oral bioavailability, anticonvulsant activity, and sedative side-effect profile of three structural analogs of KRM-II-81 (**Fig. 1**) will be disclosed. A structural basis for the reduced sedative profile of these imidazodiazepine was also elucidated. The compounds were constructed to determine changes in bioavailability and *in vivo* efficacy (anticonvulsant activity) with specific structural variation of the KRM-II-81 compound as shown in **figure 1**. FR-II-60 replaced the pyridine with a 2'-Cl phenyl group. Both KPP-III-34 and KPP-III-51 substituted the 1,3 oxazole with a 1,4 oxazole, known also to produce a non-sedating molecule like KRM-II-81 (compound 6 in Pandey et al., 2020). Ethyl substituents were added to the oxazoles as another structural change. In addition, the ethynyl group of KPP-III-51 was replaced by a bromine atom to create

KPP-III-34, allowing direct comparisons of this structural element. Since KPP-III-34 demonstrated the best brain exposure after oral gavage in rats, yielding a brain AUC value 14% higher than that of the parent KRM-II-81, as estimated as the average from two previous studies (Golani et al., 2022a; Mian et al., 2022), this compound was selected for additional more detailed anticonvulsant profiling.

JPET Fast Forward. Published on February 6, 2023 as DOI: 10.1124/jpet.122.001362
This article has not been copyedited and formatted. The final version may differ from this version.

Materials and Methods

Compounds.

FR-II-60, KPP-III-34, and KPP-III-51 were synthesized by us (JM Cook laboratory, University of Wisconsin-Milwaukee) as previously described (Knutson et al., 2020; Li et al., 2018; Pandey et al., 2020; Poe et al., 2016; Rashid, 2021). The other compounds were obtained from Sigma-Aldrich (St. Louis, MO, USA).

The test compounds were suspended in 1% carboxymethylcellulose unless otherwise noted; PTZ was dissolved in 0.9%NaCl. Compounds were dosed at 10 ml/kg in mice and 1 ml/kg in rats.

Cytotoxicity.

These studies were conducted at the University of Wisconsin-Milwaukee. The methods used cultured human embryonic kidney HEK293T cells were reported (Supplementary Information of Poe et al., 2016). 3-dibutylamino-1-(4- hexyl-phenyl)-propan-1-one (150 μM in DMSO) was used as a positive control and DMSO alone as a negative control. After 18 h incubation, cell levels were assayed.

Receptor binding.

Radioligand binding studies at the primary (benzodiazepine binding site of the $GABA_A$ receptor) and at secondary protein binding sites were conducted by the National Institute of Mental Health Psychoactive Drug Screening Program (NIMH PDSP) with 4 replicates using the methods described (Roth, 2018)(see Besnard et al. 2012 for overview of assay systems). Binding in rat brain tissue using [^{3}H]flunitrazepam was used as the primary screen as described (Chang and Snyder, 1978; Sieghart et al., 1983).

Rodent assays.

All studies were performed in accordance with guidelines of the national governments and by local animal care and use committees. All animals had free access to food and water except when they were removed from their cages for experimental procedures. All animals were group-housed in approved density housing in a temperature-, humidity-, and light-controlled vivarium prior to experimental study.

Intraperitoneal dosing - Seizure models and rotarod.

These studies were conducted by the U.S. National Institutes of Health Epilepsy Therapy Screening Program (formerly Anticonvulsant Screening Program). The assay methods used have been reported ("PANAChE current screening," n.d.; Witkin et al., 2020, 2018). The male, CF1 mice and Male, Sprague-Dawely rats, both sourced from Charles River Breeders, used in these experiments were group housed prior to experimental treatments.

In the 6 Hz (44 mA) model, the eyes of mice were treated with a drop of 0.5% tetracaine hydrochloride in 0.9% NaCl. 44 mA stimulation to induce seizures was delivered by corneal electrodes for 3s (Witkin et al., 2018). A seizure was defined as occurring if there was an initial momentary stun followed by jaw clonus, forelimb clonus, twitching of the vibrissae, and Straub tail.

In the Maximal Electroshock (MES) test, mice were given 50 mA, 60 Hz, for 0.2 s via corneal electrodes after eye treatment with 0.5% tetracaine hydrochloride.

Behavioral assessment of the mice was made after dosing with the test compound by placing them on a 1-inch knurled rod rotating at 6 r.p.m. A mouse was scored as impaired if it fell off three times during a 1 min period.

Additionally, 36 specific signs were monitored by observers blinded to treatments (e.g., salivation, hyperactivity, loss of righting, lethality).

Data are presented as the number of mice affected (protected in seizure assays or failing the rotorod test for motor-impairment assay). Fisher's Exact Probability test (one-tail) assessed statistical significance with the *a priori* prediction of increases in number of mice protected compared to the no drug treatment condition ($p<0.05$). The N value for control (no drug) condition was 12 (three dose conditions x 4 mice/dose condition). Historical controls were employed where under vehicle conditions there was neither any protection from seizures nor impairment of rotarod performances (C, Metcalf, University

of Utah, personal communication). Probit analysis was used to calculate ED_{50} and the 95% confidence interval.

Oral dose pharmacokinetics.

These experiments were conducted at the University of Belgrade, Serbia. To determine pharmacokinetic parameters and concentration-time profiles of the selected ligands, a standard pharmacokinetic study was conducted using adult male, Sprague Dawley rats (University of Belgrade, Belgrade, Serbia). Rats were housed in groups of five (21±2 °C, 40–45% relative humidity). They had free access to standard rat chow and water under a 12:12 h light/dark cycle (lights on at 06.00 h). All animal handling and testing occurred in the light phase.

The study was conducted as approved by the Ethical Council for the Protection of Experimental Animals of the Ministry of Agriculture, Forestry and Water Management of the Republic of Serbia.

The rats (n = 45, 280-320 g) were divided into three cohorts of five groups of animals; each group contained three animals corresponding to predetermined time sampling intervals (15 min, 40 min, 2 h, 6 h and 24 h). Rats received a cassette of three compounds (2.0 mg/kg, p.o.) from an 0.4 mg/ml suspension in 0.25% methyl cellulose in distilled water.

At the designated time intervals, animals were anesthetized with ketamine HCl (90 mg/kg, i.p.) (Ketamidor, Richter Pharma AG, Wels, Austria) and xylazine HCl (10 mg/kg, i.p.) (Xylased, Bioveta, A. S., Ivanovice na Hane, Czech Republic), and samples of blood (collected via cardiac puncture in heparinized syringes) and brain were taken. Plasma was obtained after centrifugation for 10 min at 1000 x g (MiniSpin® plus centrifuge, Eppendorf, Germany). Brain tissue samples were weighted and homogenized in 1 ml of methanol via ultrasonic probe sonication (70% amplitude 2 x 20 s). Supernatants were separated after centrifugation for 20 min at 3400 × g (MiniSpin® plus centrifuge). Plasma and supernatants were further processed with solid phase extraction using Oasis HLB cartridges (Waters Corporation, Milford, MA). Sample preparation and concentration determination were performed by ultraperformance liquid chromatography–tandem mass spectrometry (UPLC–MS/MS) with Thermo Scientific Accela 600 UPLC system connected to a Thermo Scientific TSQ Quantum Access MAX triple quadrupole mass spectrometer (Thermo Fisher Scientific, San Jose, California), equipped with an electrospray ionization source, as described in detail (Obradović et al., 2014). Non-compartmental pharmacokinetic analysis was performed using PK Functions for Microsoft Excel software developed by J. Usansky and colleagues (see www.pharmpk.com/xcel/pkf/pkf.doc for details and software download) Graph construction was by Sigma Plot 12 (Systat Software Inc., USA).

Oral dose – anticonvulsant effects.

Pentylenetetrazol (PTZ)-induced seizures in mice.

These studies were conducted at Indiana University, Indianapolis, IN. Male, C57BL/6N mice (Charles River, Indianapolis, IN) were used. Experimental compounds were suspended in 1% carboxymethylcellulose and PTZ was dissolved in 0.9% NaCl. Compounds were dosed at 10 ml/kg. The mice were given test compound (p.o.) and placed back into their home cages. After 60 min, these mice were given PTZ (75 mg/kg, s.c.) as described (Knutson et al. (2020). The latency to produce clonic or tonic seizures were measured by stopwatch to the second by a trained observed. The number of mice that died within the 60 min observation period was also recorded.

Latency to clonus and tonus were analyzed separately by one-way ANOVA followed by Dunnett's test (a priori probabilities of 0.05 were set for statistical significance). Lethality was statistically evaluated by Fisher's Exact Probability test at 0.05.

Pentylenetetrazol (PTZ)-induced seizures in rats.

KPP-III-34 was studied in rats as a protector against clonic convulsions induced by PTZ. Following the oral administration of KPP-III-34, PTZ was given to male, CD Sprague-Dawley IGS rats at 68 mg/kg, s.c.. An episode of approximately 3 to 5 s of clonic spasms of the fore and/or hind limbs, jaws, or vibrissae was taken as the endpoint. Animals not displaying fore and/or hind limb clonus, jaw chomping, or vibrissae twitching were considered protected. Both time course and dose-response data were collected.

Corneal kindling in mice.

In these experiments (University of Utah, Salt Lake City, UT), KPP-III-34 was evaluated for its ability to block seizures in fully-kindled mice using methods as described previously (Witkin et al., 2020). Adult, male CF1 mice (n = 8 per group, 18-25 g) were kindled to a criterion of 5 consecutive secondarily generalized seizures of stage 5 by exposure to twice daily corneal stimulation (3 mA at 60 Hz for 3 s). After reaching the first stage 5 seizure (generally after about two weeks), the twice daily stimulation regimen was continued until each mouse achieved the criteria of 5 consecutive stage 5 seizures, at which point the mouse was considered to be fully seizure kindled. Fully kindled mice continued to be stimulated every 2 to 3 days until all mice become fully kindled.

Testing of KPP-III-34 began at least 5 days after the last corneal stimulation. Compounds were dosed 1 h prior to stimulation for the assessment of anticonvulsant efficacy. Doses of 1-30 mg/kg, p.o. were tested in groups of 8 mice. The percentage of mice protected, and the seizure severity score were measured.

The effects of KPP-III-34 on seizure protection were assessed by Fisher's exact probability test and the ED_{50} and 95% confidence limits were determined by probit analysis. Effects of the compounds on seizure severity scores were analyzed by one-way ANOVA followed by Dunnett's test. Probabilities of < 0.05 were set a priori as the accepted level of statistical significance.

Mesial temporal lobe model.

Seven, male C57/Bl6 mice (10 wk old from Janvier Labs, Le-Genest-St-Isle, France) were used in these experiments conducted by Synapcell (Saint Ismier, France). Seizures were generated by unilateral application of kainic acid into the dorsal hippocampus according to standard protocol (https:/panache.ninds.nih.gov) as previously described (Witkin et al., 2020). Two to three weeks after the kainate injection, spontaneous recurrent hippocampal paroxysmal discharges were recorded in the epileptic hippocampus. The mice were allowed to recover for 4 wk prior to drug testing. Each mouse was used as its own control. Digital EEG recordings were performed on freely moving mice for 20 min prior to drug testing and then for 90 min post dosing.

KPP-III-34 (30 mg/kg) was given orally, 60 min prior to EEG recording. The number of hippocampal paroxysmal discharges were counted during baseline and drug conditions and compared by Student's t-test for paired observations. Probabilities of < 0.05 were set a priori as the accepted level of statistical significance.

Oral dose side-effect profiling.

Motor-impairment: Rotarod in mice.

Methods were generally as previously reported (Pandey et al., 2020) and were carried out at the University of Wisconsin-Milwaukee, WI. Female, Swiss Webster mice were trained to maintain balance at a constant speed of 15 rpm on the rotarod apparatus (Omnitech Electronics Inc., Nova Scotia, Canada) until they reached a behavioral criterion of successful

balance for 3 min across three consecutive trials. Separate groups of nine mice received oral gavage of vehicle (2% hydroxypropyl methylcellulose and 2.5% polyethylene glycol) or compounds in a volume of 200 μL. Diazepam in 10% DMSO, 40% propylene glycol, and 50% phosphate-buffered saline was used as a positive control at 5 mg/kg, p.o.. The mice were placed on the rotarod at three separate time points of 10, 30, and 60 minutes after administration. A 'fail' was defined for each mouse falling twice prior to 3 min.

Data were analyzed separately for each compound tested by two-way repeated-measures ANOVA with time, dose, and animals as factors. Post-hoc analyses were made by Bonferroni's multiple comparison test ($p<0.05$ set as the a priori rate for statistical significance).

Modified Irwin test in rats. KPP-III-34 that was chosen for profiling was given orally and assessed for untoward effects by previously published methods (Mathiasen and Moser, 2018). The studies were conducted at the University of Utah, Salt Lake City, UT. Before testing, animals were handled over two days to familiarize them with handling. Rats were visually evaluated by two independent observers for impaired autonomic (e.g., salivation, porphyrin), neuromuscular (e.g., ataxia, tremors), sensorimotor (e.g., hyperesthesia, loss of righting reflex), and behavioral (e.g., vocalizations, grooming) function at 0.25, 0.5, 1, 2, and 4 h post oral dosing (50-500 mg/kg) (N=8/dose). The rats were also observed 24 h after compound dosing to assess recovery from any impairment seen the previous day. A numerical score is assigned for the severity, from normal to extreme, for each functional parameter.

JPET Fast Forward. Published on February 6, 2023 as DOI: 10.1124/jpet.122.001362
This article has not been copyedited and formatted. The final version may differ from this version.

Molecular docking studies.

Studies were conducted as previously described (Golani et al., 2022b; Pandey et al., 2020; Witkin et al., 2020) at the University of Wisconsin-Milwaukee. In brief, molecular docking was performed using AutoDock Vina 1.5.6.22 and the CryoEM structure of the human full-length α1β3γ2L GABAAR ion complex with alprazolam (PDB: 6HUO) (Masiulis et al., 2019). FR-II-60 and KPP-III-34 were so modeled. The docking analysis of KPP-III-51 was reported previously (Pandey et al., 2020).

JPET Fast Forward. Published on February 6, 2023 as DOI: 10.1124/jpet.122.001362
This article has not been copyedited and formatted. The final version may differ from this version.

Results

Cytotoxicity. 3-dibutylamino-1-(4- hexyl-phenyl)-propan-1-one was run as a positive control at 150 μM; all cells were killed at this concentration. For FR-II-60, the IC_{50} was >150 μM and for KPP-III-34 and KPP-III-51, the IC_{50} was > 300 μM for cytotoxicity in HEK 293 cells.

Receptor Binding. The inhibition of radioligand binding is shown in **Table 1**. Only the receptor proteins for which binding was inhibited by >50% at 10 μM across 47 receptor targets (including hERG for potential cardiovascular liability) in the primary screen are shown; the values for 5-HT_{1A} and peripheral benzodiazepine receptor (PBR) are reported here for purposes of comparison to the other analogs.

Intraperitoneal Dosing – Seizure models and rotarod.

Intraperitoneal dosing with FR-II-60, KPP-III-34, and KPP-III-51 was studied in two seizure models in mice at 0.5 h and 2 h post dosing. The mice were also tested for motor impairment as measured on a rotarod to ascertain the impact of the compounds on the ability of the mice to maintain balance. The data are summarized in **Table 2**. Dose-dependent increases in the number of mice protected from seizures were observed for FR-II-60 and for KPP-III-34 but not for KPP-III-51 where no dose produced significant protection. The doses that produced seizure protection were also generally motorically

impairing as assessed on the rotarod for FR-II-60 and KPP-III-51. In contrast KPP-III-34 protected against seizures induced by 6 Hz stimulation at 100 mg/kg without significantly impairing rotarod performance.

All mice were observed for atypical body signs including sedation, ataxia, parasympathetic activity, seizures, tremor, and death. No adverse reactions were noted at either the 0.5 or 2 h time points except for KPP-III-51 where mice had difficulty grasping the rotarod at 300 mg/kg at 0.5 h post dosing. There was no mortality at 72 h post dosing in any of the mice dosed with the exception of one mouse in the 100 mg/kg group for KPP-III-51 that died during the MES test (**Table 2**).

A further study of the anticonvulsant effects of KPP-III-34 was conducted in rats with i.p. doses of 10-25 mg/kg KPP-III-34 with 8 rats/dose (0.25 h post dosing with KPP-III-34). Using s.c. PTZ as a chemoconvulsant, the ED_{50} of KPP-III-34 was 16.6 mg/kg (95% Cl: 13.6-19.0 mg/kg). In the rotarod assay in rats conducted at 0.5 h post dosing in 8 rats each at doses of 50-100 mg/kg, i.p., the ED_{50} for disruption of performances was 77.4 mg/kg (95% Cl: 62.6 – 91.0 mg/kg). The differential of motororic effects vs. anaticonvulsant efficacy was thus 4.7.

Oral Dose Pharmacokinetics.

JPET Fast Forward. Published on February 6, 2023 as DOI: 10.1124/jpet.122.001362
This article has not been copyedited and formatted. The final version may differ from this version.

Pharmacokinetic studies were performed in order to evaluate the *in vivo* fate, after oral gavage, of the three structural analogs of KRM-II-81 (FR-II-60, KPP-III-34, and KPP-III-51). Kinetic profiles in plasma and brain for FR-II-60 (**Fig. 2**), KPP-III-34 (**Fig. 3**), and KPP-III-51 (**Fig. 4**) show similarities and some striking differences. Using the compound concentration summary parameters of C_{max} and $AUC_{0–24}$ (**Table 3**), the plasma levels achieved by KPP-III-34 are up to ten-fold greater than that of the two other analogs. Likewise, the brain exposures achieved by KPP-III-34 ($AUC_{0–24}$) are more than two-fold higher than the other two analogs, and 14% higher than that with KRM-II-81 (Golani et al., 2022a; Mian et al., 2022). The C_{max} for brain levels of KPP-II-51 was much lower than that of the other two analogs. However, given the sustained increases in brain levels of KPP-III-51 (**Fig. 4**) compared to the other two analogs, the AUC differences are not as great.

It is also noted that whereas FR-II-60 displayed relatively linear kinetics (**Fig. 2**), KPP-III-34 (**Fig. 3**) and KPP-III-51 (**Fig. 4**) showed higher levels of compound in brain than plasma at 24 h. Compound concentrations from these studies converted from weight to molar units are shown in **Table 3** for direct comparison. Partition coefficients, i.e., brain to plasma ratios of compound exposure, document the larger brain to plasma uptake of FR-II-60 compared to the other compounds (**Table 3**). The large brain/plasma partition coefficient for FR-II-60 is accounted for by the high brain levels achieved compared to plasma (with variability) at 2-6 h post dosing (**Fig. 2**).

Oral Dosing – PTZ seizures in mice

FR-II-60 significantly increased the latency of PTZ to produce clonic seizures in mice ($F_{2,16}$ = 33.6, P < 0.0001). Post-hoc Dunnett's test revealed that doses of 10 and 30 mg/kg both significantly increased clonic seizure latency (**Fig. 5, left panels**). Tonic seizure latency was also significantly increased by FR-II-60 ($F_{2,13}$ = 35.7, P < 0.0001). Post-hoc Dunnett's tested revealed that both 10 and 30 mg/kg significantly increased tonic seizure latency (**Fig. 5, right panels**).

KPP-III-34 also significantly increased the latency to clonus ($F_{2,20}$ = 4.68; P = 0.023) and tonus ($F_{2,21}$ = 9.13; P = 0.002). Only the 30 mg/kg dose of KPP-III-34 significantly increased seizure latencies (**Fig. 5**).

KPP-III-51 significantly increased the latency for PTZ to induce clonic seizures ($F_{2,20}$ = 14.4; P = 0.0002) and tonic seizures ($F_{2,21}$ = 6.54; P = 0.007). Whereas only 10 mg/kg significantly increased the latency to produce clonus, both 10 and 30 mg/kg significantly increased the latency for PTZ to induce tonus (**Fig. 5**). The increases in latency to produce tonus by KPP-III-51 were also generally less than those increases produced by FR-II-60 and KPP-III-34.

All three compounds significantly prevented or exhibited trends toward preventing PTZ-induced lethality (**Table 4**). This effect was not always dose dependent. In contrast to FR-II-60 and KPP-III-34, KPP-III-51 was less efficacious on this measure.

KPP-III-34: Oral anticonvulsant activity in rats.

Based upon the preceding findings, KPP-III-34 was chosen as a compound for further anticonvulsant screening. In these studies with rats, there were no signs of impairment by KPP-III-34 and no deaths. Blockade of pentylenetetrazol-induced convulsions was dose- and time-dependent (**Table 5**). Dose-response data for orally administered KPP-III-34 are shown in **Table 6** (testing at 0.5 h post dosing of KPP-III-34). The data from the dose-response curve when dosed 0.5 h prior to PTZ yielded an ED_{50} of 15.5 mg/kg with 95% confidence limits of 8.75-25.0.

High oral doses of KPP-III-34 (50, 100, 300, 500 mg/kg) were given to rats (N = 8/group) under observation in a modified Irwin test. There were no observed signs of untoward effects at any of the time points evaluated (0.25, 0.5, 1, 2, 4, and 8 h) and no observations at 24 h post dosing of KPP-III-34 (data not shown). Further, no adverse events or lethality were observed in the rats in a functional test battery that observed autonomic, neuromuscular, sensorimotor, and behavioral functions (data not shown).

KPP-III-34: Oral dose anticonvulsant activity in the 6 Hz (44mA) assay in mice.

Effects of KPP-III-34 were studied in mice using 6 Hz (44mA) electrical stimulation to induced seizure. At doses of 50-300 mg/kg (N=8 mice/dose) given 1 h prior to 6 Hz stimulation, the ED_{50} for blocking seizures was 115.5 mg/kg with 95% confidence limits of 62.0 -177 mg/kg. In contrast, the ED_{50} for rotarod impairment was calculated to be > 300 mg/kg with the mice affected only at 300 mg/kg (2 of 8).

KPP-III-34: Oral dose anticonvulsant activity in corneal-kindled mice.

Mice that were seizure kindled by daily electrical corneal stimulation, were tested with KPP-III-34 (**Table 7**). Oral doses of KPP-III-34 dose-dependently reduced the incidence of seizures in these mice ($F_{4,39} = 7.17$, $p < 0.001$) with an ED_{50} of 12.7 mg/kg (95% confidence limits: 4.35-21.9).

KPP-III-34: Oral dose anticonvulsant activity in the mesial temporal lobe model in mice.

In the mesial temporal lobe epilepsy model, KPP-III-34 significantly reduced the number of spontaneous recurrent hippocampal paroxysmal discharges when given at 30 mg/kg, p.o. ($t_6 = 2.74$, $p = 0.034$) (**Fig. 6**).

Oral dose motor-impairment: rotarod.

Mice trained to balance on the rotarod for 3 min were given diazepam, FR-II-60, or KPP-III-34. Rotarod data for KPP-III-51 has been disclosed recently where an oral dose of 120 mg/kg did not significantly disrupt motor performance (Pandey et al., 2020).

FR-II-60 (p.o.) was studied alongside 5 mg/kg diazepam, p.o (**Fig. 7**). In this experiment there was a significant effect of drug treatment ($F_{4,80} = 6.91$; $P = 0.0003$), of time ($F_{2,80} = 4.75$; $P = 0.011$), and of subjects ($F_{40,80} = 3.63$; $P < 0.0001$) but not an overall significant treatment x time interaction ($F_{8,80} = 1.72$; $P = 0.11$). Post-hoc analyses documented a significant effect of diazepam at 10- and 30-min post dosing. Significant impairment at 80 mg/kg FR-II-60 was also observed at 10- and 30-min post dosing (**Fig. 7**).

Effects of KPP-III-34 (**Fig. 7**) showed a toward a trend toward an effect of dose ($F_{3,64} = 2.29$; $P = 0.097$), an effect of time ($F_{2,64} = 4.38$; $P = 0.017$), and a significant dose x time interaction ($F_{6,64} = 2.29$; $P = 0.046$), but not a significant effect of subjects ($F_{32,64} = 1.00$; $P = 0.49$). The effect of 120 mg/kg KPP-III-34 showed a significant effect of dose only at the 10 min time point. Effects of no other doses significantly separated from vehicle (**Fig. 7**).

Molecular docking studies.

The minimal effects of the three test compounds on rotorod performances and in visual observations encouraged molecular docking studies to help to define a structural basis. Docking experiments with KPP-III-51 have been reported (Pandey et al., 2020). Comparison of the docking of FR-II-60 and the sedating compound alprazolam are shown in **Figure 8**. Docking results from the modeling experiments indicated that replacing the C8 chlorine atom in alprazolam, with the ethynyl group in FR-II-60 leads to a loss in this key halogen bond interaction with α1His102. The docking score of FR-II-60 (**Table 8**) also indicates that the binding affinity of FR-II-60 should be less as compared to alprazolam at the α1subtype GABAAR.

Alprazolam forms a crucial halogen bond interaction between the carbonyl oxygen atom of the α1His102 backbone and the chlorine atom. The angle between the oxygen, chlorine, and carbon atoms is 167º. KPP-III-34 was docked into the CryoEM structure (**Figure 9 A and B**). The docking pose shows that the angle between oxygen, bromine and carbon atoms is 122.75º. The docking score of KPP-III-34 (**Table 8**) also indicates that the binding affinity of KPP-III-34 should be less compared to alprazolam at the α1subtype GABAAR. This was found to be the case (**Table 8**).

With the exception of the halogen bond interaction, other interactions with the α1 subunit were maintained by the predicted binding poses of FR-II-60 and KPP-III-34. Here we show that the predicted binding pose of FR-II-60 overlapped with that of alprazolam better than the predicted binding pose of KPP-III-34 (**Fig. 8B, 9B**). This predicted

interaction is consistent with the greater impairment in rotarod performances observed with FR-II-60 (**Fig. 7**). Indeed, KPP-III-34 was not sedating in rats up to 500 mg/kg, p.o. (data presented here). The disorientation of the diazepine ring, which occurs in the predicted binding pose of KPP-III-34, is probably due to compensation for the binding of the ethyl substituted oxazole ring that allows the ligand to fit in the binding pocket (**Fig. 9**). Also, the Br atom of KPP-III-34 in place of the ethynyl moiety of KPP-III-51 (**Table 8**) enables reduced binding interaction due to length differences of these two substituents.

JPET Fast Forward. Published on February 6, 2023 as DOI: 10.1124/jpet.122.001362
This article has not been copyedited and formatted. The final version may differ from this version.

Discussion

The imidazodiazepine, KRM-II-81, is undergoing preparations for clinical development (Witkin et al., 2022). In the present set of experiments, three novel analogs were synthesized to broadly test effects of specific structural features on pharmacokinetics and *in vivo* activity.

All compounds bound to brain receptors labeled by [^{3}H]-flunitrazepam (benzodiazepine binding site on the $GABA_A$ receptor). Non-GABA binding was observed at only a few of the 47 other receptors evaluated and, with one exception, binding at these non-GABA sites was weaker than at $GABA_A$ receptors. The three analogs also presented with low potency cytotoxicity with selectivity over [^{3}H]-flunitrazepam binding. Binding to hERG channels, another potential marker of *in vivo* toxicity was also weak with binding for all compounds greater than 10 μM.

The most striking findings observed with structural modifications of KRM-II-81 were the reduced systemic exposures after oral administration for FR-II-60 and KPP-III-51. One factor affecting pharmacokinetics is compound lipophilicity (Lipinski, 2004). The CLogP values for the compounds were 1.58 (KRM-II-81), 3.05 (FR-II-60), 2.38 (KPP-III-51), and 2.97 (KPP-III-34). The substantial increase in CLogP in FR-II-60 might therefore be one factor responsible for the reduction in plasma and, to a lesser degree, brain exposures relative to KRM-II-81. Theoretically, such a difference is expected to deteriorate the absorption at the level of intestinal barrier, while enhancing at the same

time its capability to pass the blood-brain barrier. Indeed, the variations in lipophilicity do appear to have some impact on the oral pharmacokinetics of these compounds. However, the substitution of a Br atom in KPP-III-34 for the ethynyl group in KPP-III-51, re-instated plasma exposures to near the levels of KRM-II-81 (**Table 9**), despite the increased lipophilicity of KPP-III-34. The dynamics regulating this difference in the two compounds will require detailed study of drug disposition, in particular, the role of metabolism.

A second peak of exposure at 24 h was also observed with KPP-III-34 suggesting a potential depot effect. This might have resulted from unpredicted precipitation in the gastrointestinal tract, even though a standard vehicle for oral dosing in preclinical animal models was chosen. It seems more probable that enterohepatic recirculation, with continuous KPP-III-34 reabsorption following biliary excretion (Zhang et al., 2021) may have taken place; however, this hypothesis needs to be experimentally investigated.

Intraperitoneal administration of FR-II-60 and KPP-III-34, but not that of KPP-III-51, produced anticonvulsant activity (6 Hz model and maximal electroshock) at doses lower than those required to disrupt rotarod performance of mice. Further investigation of KPP-III-34 showed that it was also an effective anticonvulsant (vs. PTZ) in rats by the intraperitoneal route. Oral administration of all three compounds was anticonvulsant in mice against PTZ-induced seizures and lethality, an effect also shared by KRM-II-81 (Witkin et al., 2018). However, KPP-III-51 was the weakest anticonvulsant in this assay with a lack of dose-dependence and a reduced efficacy against tonic seizures. However,

that the relatively low brain and especially plasma exposure of KPP-III-51 was sufficient to drive oral anticonvulsant activity is consistent with the ability of other imidazodiazepines, like HZ-166, to be anticonvulsant despite low exposure levels (Rivas et al., 2009). HZ-166 is the precursor molecule for KRM-II-81. An ester group in the position of the oxazole of KRM-II-81 was a target for metabolism that resulted in low bioavailability (Poe et al., 2016) and in some cases, a lack of anticonvulsant activity (Witkin et al., 2018).

Although FR-II-60 and KPP-III-51 showed marked reductions in plasma and, to a lesser extent, brain exposure after oral administration compared to KRM-II-81, they were still able to produce anticonvulsant effects. This suggests potentially important features of these compounds as antiepileptics since lower plasma exposures generating therapeutic efficacy should be associated with larger margins of safety. In this vein, the pharmacokinetic behavior of KPP-III-51 and FR-II-60 cannot be seen as inadequate for their possible further development as brain targeting treatments.

We suggest that the anticonvulsant activity of the compounds is due to their ability to act as GABAkines (potentiators) of GABAARs. The brain exposures of the compounds in rats after oral administration were compared to their affinities for binding to rat brain benzodiazepine receptors. The C_{max} level of exposure was greater than the IC_{50} for FR-II-60 (11.5 times) and KPP-III-34 (5.5 times), but not KPP-III-51 (0.4 times). But the pharmacokinetic data were obtained after oral administration of only 2 mg/kg whereas higher oral doses were used in the anticonvulsant studies. Although

ancillary activity (**Table 1**) might be responsible or contribute, we view this as unlikely due to low potency. Kappa opioid receptor agonists have been shown to be anticonvulsant (Loacker et al., 2007; Manocha et al., 2003; Zangrandi and Schwarzer, 2022). Peripheral benzodiazepine receptor ligands have also shown potential relationships toward seizure control (Ferrarese et al., 1997; Shiotani et al., 2000) as have 5-HT_{1A} receptors (Gharib et al., 2018; Pelz et al., 2017; Sapa et al., 2014; Waszkielewicz et al., 2015)(Gharib et al., 2018; Pelz et al., 2017; Sapa et al., 2014; Waszkielewicz et al., 2015). However, the selectivity of these compounds over these targets is one piece of evidence that these ancillary actions are not necessary for the anticonvulsant activity of these compounds. Nonetheless, the possibility that multiple actions contribute to anticonvulsant efficacy cannot be excluded with these data alone.

KPP-III-34 was selected for additional anticonvulsant profiling based upon its encouraging brain exposure after oral gavage and anticonvulsant data. In addition to protecting against PTZ-induced seizures and lethality in mice, KPP-III-34, like KRM-II-81 (Witkin et al., 2020, 2018), was an efficacious anticonvulsant against PTZ in rats, and against fully kindled seizures (corneal kindled seizures in mice), as well in a kainate-induced mouse model of mesial temporal lobe epilepsy. The 6 Hz (44mA), corneal kindling, and mesial temporal lobe models are all used to help identify improved anticonvulsants and those that might function against pharmacoresistant epilepsy (Barton et al., 2001; Bouilleret et al., 1999; Leclercq et al., 2014; Rowley and White, 2010; Wilcox et al., 2013).

The three analogs of KRM-II-81 did not show appreciable sensorimotor impairment in mice when measured on the rotarod; in contrast diazepam disrupted performances. The ability of benzodiazepine GABAkines to produce sedative effects and decreases in locomotion in rodents is well documented (c.f., Knutson et al., 2021; Witkin et al., 2018). In comparison, when tested up to 500 mg/kg in rats, p.o., KPP-III-34 did not exhibit any signs indicative of untoward effects. These findings are congruent with the reduced impact of imidazodiazepines of this series on sensorimotor function including HZ-166 and KRM-II-81 (c.f., (Cerne et al., 2022; Witkin et al., 2020; 2022). As with KPP-II-51 which also demonstrated low sensorimotor impairing effects (Pandey et al., 2020), FR-II-60 and KPP-III-34 showed weaker halogen bonding with the backbone of α1His102. The ideal bond angle for a halogen bond is 180º; the halogen bond becomes weaker if the angle deviates from linear (Shinada et al., 2019). Consequently, KPP-III-34 forms a weaker halogen bond with the backbone of α1His102. This could be the reason for the decreased affinity towards α1, which results in no sedation of KPP-III-34 up to 120 mg/kg in mice. KPP-III-34 was also devoid of notable side-effects when given up to 500 mg/kg in rats. The ethyl oxazole, KPP-III-34, was less sedating and ataxic than FR-II-60 and related oxazoles because the former ethyl oxazole fits into the binding pocket with a slightly different alignment, which decreased the strength of the halogen bond of the C-8 bromine atom with the histidine backbone of the C-loop (see Golani et al., 2022b).

That these three novel imidazodiazepine GABAkines displayed oral bioavailability and anticonvulsant efficacy with low propensity to disrupt sensorimotor function or produce other untoward side-effects is encouraging of further development. The comparative

pharmacology of KPP-III-34 relative to the parent molecule KRM-II-81 is summarized in **Table 9**. Small decreases in systemic plasma exposure were observed with KPP-III-34 but the brain levels and brain to plasma ratio of this analog was generally unharmed. Although equally efficacious to KRM-II-81, the oral anticonvulsant potency of KPP-III-34 was slightly less than that of KRM-II-81. Both compounds demonstrated good tolerability in mice and rats that corresponded to their molecular modelling docking scores with the brominated KPP-III-34 molecule showing the least interaction with the critical α1 residue. KPP-III-34 at GABAARs was more potent than that of KRM-II-81 but KPP-III-34 also incurred additional low-potency off-target activity compared to KRM-II-81. Thus, KPP-III-34 presents as a novel compound with overlapping as well as unique pharmacological properties that continues to carry anticonvulsant activity with low sedative liability.

Footnotes

[1]We are grateful to the generous support from Henry and Nellie Pence Foundation for their support of this research that has enabled the advancement of new potential therapeutic entities. We also acknowledge the UW-Milwaukee Shimadzu Laboratory for Advanced and Applied Analytical Chemistry and support from the Milwaukee Institute of Drug Discovery and the University of Wisconsin-Milwaukee Research Foundation. Additional funding was provided as noted here. National Institutes of Health (NIH): DA-043204 and NS-076517; National Science Foundation (NSF), Division of Chemistry: CHE-1625735; Ministry of Education, Science and Technological Development, Republic of Serbia through Grant Agreement with University of Belgrade-Faculty of Pharmacy No: 451-03-9/2021-14/200161.

JPET Fast Forward. Published on February 6, 2023 as DOI: 10.1124/jpet.122.001362
This article has not been copyedited and formatted. The final version may differ from this version.

Authorship Contributions

Participated in research design: Pandey K, Savic M, Divović B, Golani L, Witkin J, Ping X, Cook J

Conducted experiments: Pandey K, Rashid F, Divović B, Golani L, Ping X

Contributed new reagents or analytic tools: Pandey K, Rashid F, Golani L

Performed data analysis: Divović B, Golani L, Ping X, Witkin J, Savic M

Wrote or contributed to the writing of the manuscript: Pandey K, Divović B, Rashid F, Golani LK, Cerne R, Zahn NM, Meyer MJ, Arnold LA, Sharmin D, Mian Md Y, Smith JL, Ping X, Jin X, Lippa A, Tiruveedhula VVNPB, Cook JM, Savić MM, Witkin JM

REFERENCES

Barton ME, Klein BD, Wolf HH, and White HS (2001) Pharmacological characterization of the 6 Hz psychomotor seizure model of partial epilepsy. Epilepsy Res 47: 217–227.

Besnard J, Ruda GF, Setola V, Abecassis K, Rodriguiz RM, Huang XP, Norval S, Sassano MF, Shin AI, Webster LA, Simeons FR, Stojanovski L, Prat A, Seidah NG, Constam DB, Bickerton GR, Read KD, Wetsel WC, Gilbert IH, Roth BL, Hopkins AL. Automated design of ligands to polypharmacological profiles. Nature. 2012 Dec 13;492(7428):215-20. doi: 10.1038/nature11691. PMID: 23235874; PMCID: PMC3653568.

Biggerstaff, A., Kivell, B., Smith, J.L., Mian, M.Y., Golani, L.K., Rashid, F., Sharmin, D., Knutson, D.E., Cerne, R., Cook, J.M., Witkin, J.M., 2020. The α2,3-selective potentiators of GABAA receptors, KRM-II-81 and MP-III-80, produce anxiolytic-like effects and block chemotherapy-induced hyperalgesia in mice without tolerance development. Pharmacol Biochem Behav 196, 172996. https://doi.org/10.1016/j.pbb.2020.172996

Bouilleret V, Ridoux V, Depaulis A, Marescaux C, Nehlig A, and Le Gal La Salle G (1999) Recurrent seizures and hippocampal sclerosis following intrahippocampal kainate injection in adult mice: electroencephalography, histopathology and synaptic reorganization similar to mesial temporal lobe epilepsy. Neuroscience 89: 717–729.

Cerne, R., Lippa, A., Poe, M.M., Smith, J.L., Jin, X., Ping, X., Golani, L.K., Cook, J.M., Witkin, J.M., 2021. GABAkines - Advances in the discovery, development, and commercialization of positive allosteric modulators of GABAA receptors. Pharmacol Ther 108035. https://doi.org/10.1016/j.pharmthera.2021.108035

Cerne, R., Smith, J.L., Fisher, J.L., Golani, L.K., Knutson, D.E., Cook, J.M., Witkin, J.M., 2022. Chapter 11 - The orally bioavailable imidazodiazepine, KRM-II-81, is a novel potentiator of α2/3-containing GABAA receptors with analgesic efficacy, in: Rajendram, R., Patel, V.B., Preedy, V.R., Martin, C.R. (Eds.), The Neurobiology, Physiology, and Psychology of Pain. Academic Press, pp. 117–127. https://doi.org/10.1016/B978-0-12-820589-1.00011-7

Chang, R.S., Snyder, S.H., 1978. Benzodiazepine receptors: labeling in intact animals with [3H] flunitrazepam. Eur J Pharmacol 48, 213–218. https://doi.org/10.1016/0014-2999(78)90330-8

FDA-CDER, 2022. FDA approves drug for treatment of seizures associated with rare disease in patients two years of age and older [WWW Document]. FDA. URL https://www.fda.gov/drugs/news-events-human-drugs/fda-approves-drug-treatment-seizures-associated-rare-disease-patients-two-years-age-and-older (accessed 3.28.22).

Ferrarese, C., Tortorella, R., Bogliun, G., Beghi, E., Cogliati, T., Zoia, C., Passoni, D., Frattola, L., 1997. Decreased density of lymphocyte benzodiazepine receptors in drug-resistant epileptic patients. Epilepsy Res 27, 181–185. https://doi.org/10.1016/s0920-1211(97)01035-8

Gharib, A., Sayyahi, Z., Komaki, A., Barkley, V., Sarihi, A., Mirnajafi-Zadeh, J., 2018. The role of 5-HT1A receptors of hippocampal CA1 region in anticonvulsant effects of low-frequency stimulation in amygdala kindled rats. Physiol Behav 196, 119–125. https://doi.org/10.1016/j.physbeh.2018.08.025

Golani, L. K., Divović, B., Sharmin, D., Pandey, K. P., Mian, M. Y., Cerne, R., Zahn, N. M., Meyer, M. J., Tiruveedhula, V., Smith, J. L., Ping, X., Jin, X., Lippa, A., Schkeryantz, J. M., Arnold, L. A., Cook, J. M., Savić, M. M., & Witkin, J. M. (2022). Metabolism, pharmacokinetics, and anticonvulsant activity of a deuterated analog of the α2/3-selective GABAkine KRM-II-81. *Biopharmaceutics & drug disposition*, *43*(2), 66–75. https://doi.org/10.1002/bdd.2313

Golani, L. K., Yeunus Mian, M., Ahmed, T., Pandey, K. P., Mondal, P., Sharmin, D., Rezvanian, S., Witkin, J. M., & Cook, J. M. (2022). Rationalizing the binding and α subtype selectivity of synthesized imidazodiazepines and benzodiazepines at GABAA receptors by using molecular docking studies. *Bioorganic & medicinal chemistry letters*, *62*, 128637. https://doi.org/10.1016/j.bmcl.2022.128637

Klepner, C.A., Lippa, A.S., Benson, D.I., Sano, M.C., Beer, B., 1979. Resolution of two biochemically and pharmacologically distinct benzodiazepine receptors. Pharmacol. Biochem. Behav. 11, 457–462. https://doi.org/10.1016/0091-3057(79)90125-4

Knutson, D.E., Smith, J.L., Ping, X., Jin, X., Golani, L.K., Li, G., Tiruveedhula, V.V.N.P.B., Rashid, F., Mian, M.Y., Jahan, R., Sharmin, D., Cerne, R., Cook, J.M., Witkin, J.M., 2020. Imidazodiazepine Anticonvulsant, KRM-II-81,

Produces Novel, Non-diazepam-like Antiseizure Effects. ACS Chem Neurosci 11, 2624–2637. https://doi.org/10.1021/acschemneuro.0c00295

Mian MY, Divović B, Sharmin D, Pandey KP, Golani LK, Tiruveedhula VVNPB, Cerne R, Smith JL, Ping X, Jin X, Imler GH, Deschamps JR, Lippa A, Cook JM, Savić MM, Rowlett J, Witkin JM. Hydrochloride Salt of the GABAkine KRM-II-81. ACS Omega. 2022 Jul 27;7(31):27550-27559. doi: 10.1021/acsomega.2c03029. PMID: 35967038; PMCID: PMC9366947.

Leclercq K, Matagne A, and Kaminski RM (2014) Low potency and limited efficacy of antiepileptic drugs in the mouse 6 Hz corneal kindling model. Epilepsy Res 108: 675–683.

Lewter, L.A., 2019. Characterization of novel α2/α3 subtype-selective GABAA receptor positive allosteric modulators. A dissertation submitted to the faculty of the Graduate School of the University at Buffalo, The State University of New York, Buffalo, NY.

Li, G., Golani, L.K., Jahan, R., Rashid, F., Cook, J.M., 2018. Improved Synthesis of Anxiolytic, Anticonvulsant, and Antinociceptive α2/α3-GABA(A)-ergic Receptor Subtype Selective Ligands as Promising Agents to Treat Anxiety, Epilepsy, and Neuropathic Pain. Synthesis 50, 4124–4132. https://doi.org/10.1055/s-0037-1610211

Lipinski C. A. (2004). Lead- and drug-like compounds: the rule-of-five revolution. *Drug discovery today. Technologies*, *1*(4), 337–341. https://doi.org/10.1016/j.ddtec.2004.11.007

Lippa, A.S., Beer, B., Sano, M.C., Vogel, R.A., Meyerson, L.R., 1981. Differential ontogeny of type 1 and type 2 benzodiazepine receptors. Life Sci 28, 2343–2347. https://doi.org/10.1016/0024-3205(81)90498-7

Lippa, A.S., Klepner, C.A., Yunger, L., Sano, M.C., Smith, W.V., Beer, B., 1978. Relationship between benzodiazepine receptors and experimental anxiety in rats. Pharmacol Biochem Behav 9, 853–856. https://doi.org/10.1016/0091-3057(78)90368-4

Lippa, A.S., Meyerson, L.R., Beer, B., 1982. Molecular substrates of anxiety: clues from the heterogeneity of benzodiazepine receptors. Life Sci 31, 1409–1417. https://doi.org/10.1016/0024-3205(82)90001-7

Loacker, S., Sayyah, M., Wittmann, W., Herzog, H., Schwarzer, C., 2007. Endogenous dynorphin in epileptogenesis and epilepsy: anticonvulsant net effect via kappa opioid receptors. Brain 130, 1017–1028. https://doi.org/10.1093/brain/awl384

Manocha, A., Mediratta, P.K., Sharma, K.K., 2003. Studies on the anticonvulsant effect of U50488H on maximal electroshock seizure in mice. Pharmacol Biochem Behav 76, 111–117. https://doi.org/10.1016/s0091-3057(03)00218-1

Masiulis, S., Desai, R., Uchański, T., Martin, I.S., Laverty, D., Karia, D., Malinauskas, T., Zivanov, J., Pardon, E., Kotecha, A., Steyaert, J., Miller, K.W., Aricescu, A.R., 2019. GABA A receptor signalling mechanisms revealed by structural pharmacology. Nature 565, 454. https://doi.org/10.1038/s41586-018-0832-5

Mathiasen, J.R., Moser, V.C., 2018. The Irwin Test and Functional Observational Battery (FOB) for Assessing the Effects of Compounds on Behavior, Physiology, and Safety Pharmacology in Rodents. Curr Protoc Pharmacol 83, e43. https://doi.org/10.1002/cpph.43

Methuku, K.R., Li, X., Cerne, R., Gleason, S.D., Schkeryantz, J.M., Tiruveedhula, V.V.N.P.B., Golani, L.K., Li, G., Poe, M.M., Rahman, Md.T., Cook, J.M., Fisher, J.L., Witkin, J.M., 2018. An antidepressant-related pharmacological signature for positive allosteric modulators of α2/3-containing GABAA receptors. Pharmacology Biochemistry and Behavior 170, 9–13. https://doi.org/10.1016/j.pbb.2018.04.009Mian, M. Y., Divović, B., Sharmin, D., Pandey, K. P., Golani, L. K., Tiruveedhula, V., Cerne, R., Smith, J. L., Ping, X., Jin, X., Imler, G. H., Deschamps, J. R., Lippa, A., Cook, J. M., Savić, M. M., Rowlett, J., & Witkin, J. M. (2022). Hydrochloride Salt of the GABAkine KRM-II-81. *ACS omega*, *7*(31), 27550–27559. https://doi.org/10.1021/acsomega.2c03029

Moerke, M.J., Li, G., Golani, L.K., Cook, J., Negus, S.S., 2019. Effects of the α2/α3-subtype-selective GABAA receptor positive allosteric modulator KRM-II-81 on pain-depressed behavior in rats: comparison with ketorolac and diazepam. Behav Pharmacol 30, 452–461. https://doi.org/10.1097/FBP.0000000000000464

Obradović, A.L., Joksimović, S., Poe, M.M., Ramerstorfer, J., Varagic, Z., Namjoshi, O., Batinić, B., Radulović, T., Marković, B., Roth, B.L., Sieghart, W., Cook, J.M., Savić, M.M., 2014. Sh-I-048A, an in vitro non-selective super-agonist at the benzodiazepine site of GABAA receptors: the approximated activation of receptor

subtypes may explain behavioral effects. Brain Res 1554, 36–48. https://doi.org/10.1016/j.brainres.2014.01.036

PANAChE current screening [WWW Document], n.d. URL https://panache.ninds.nih.gov/Home/CurrentModels (accessed 3.25.22).

Pandey, K.P., Khan, Z.A., Golani, L.K., Mondal, P., Mian, Y., Rashid, F., Tiruveedhula, V.V.N.P.B., Knutson, D.E., Sharmin, D., Ahmed, T., Rezvanian, S., Zahn, N.M., Arnold, L.A., Witkin, J.M., Cook, J.M., 2020. Design, synthesis and characterization of novel gamma-aminobutyric acid type A receptor ligands. ARKIVOC 2020, 242–256. https://doi.org/10.24820/ark.5550190.p011.398

Pelz, M.C., Schoolcraft, K.D., Larson, C., Spring, M.G., López, H.H., 2017. Assessing the role of serotonergic receptors in cannabidiol's anticonvulsant efficacy. Epilepsy Behav 73, 111–118. https://doi.org/10.1016/j.yebeh.2017.04.045

Poe, M.M., Methuku, K.R., Li, G., Verma, A.R., Teske, K.A., Stafford, D.C., Arnold, L.A., Cramer, J.W., Jones, T.M., Cerne, R., Krambis, M.J., Witkin, J.M., Jambrina, E., Rehman, S., Ernst, M., Cook, J.M., Schkeryantz, J.M., 2016. Synthesis and characterization of a novel gamma-aminobutyric acid type A (GABAA) receptor ligand that combines outstanding metabolic stability, pharmacokinetics, and anxiolytic efficacy. J Med Chem 59, 10800–10806. https://doi.org/10.1021/acs.jmedchem.6b01332

Rashid, F., 2021. Design and Synthesis of Achiral and Chiral Benzodiazepines and Imidazodiazepine to Modulate the Activity of GABAA Receptors for the Treatment of Cancer, CNS disorders and Pain., PhD dissertation. ed. University of Wisconsin-Milwaukee, Milwaukee, WI.

Rivas, F.M., Stables, J.P., Murphree, L., Edwankar, R.V., Edwankar, C.R., Huang, S., Jain, H.D., Zhou, H., Majumder, S., Sankar, S., Roth, B.L., Ramerstorfer, J., Furtmüller, R., Sieghart, W., Cook, J.M., 2009. Antiseizure activity of novel gamma-aminobutyric acid (A) receptor subtype-selective benzodiazepine analogues in mice and rat models. J. Med. Chem. 52, 1795–1798. https://doi.org/10.1021/jm801652d

Roth, B.L., 2018. ASSAY PROTOCOL BOOK - Version III [WWW Document]. National Institute of Mental Health Psychoactive Drug Screening Program (NIMH PDSP). URL https://pdsp.unc.edu/pdspweb/content/PDSP%20Protocols%20II%202013-03-28.pdf (accessed 3.26.22).

Sapa, J., Zygmunt, M., Kulig, K., Malawska, B., Dudek, M., Filipek, B., Bednarski, M., Kusak, A., Nowak, G., 2014. Evaluation of anticonvulsant activity of novel pyrrolidin-2-one derivatives. Pharmacol Rep 66, 708–711. https://doi.org/10.1016/j.pharep.2014.02.014

Shinada, N.K., de Brevern, A.G., Schmidtke, P., 2019. Halogens in Protein-Ligand Binding Mechanism: A Structural Perspective. J Med Chem 62, 9341–9356. https://doi.org/10.1021/acs.jmedchem.8b01453

Shiotani, T., Nakamoto, Y., Watabe, S., Yoshii, M., Nabeshima, T., 2000. Anticonvulsant actions of nefiracetam on epileptic EL mice and their relation to peripheral-type benzodiazepine receptors. Brain Res 859, 255–261. https://doi.org/10.1016/s0006-8993(00)01971-5

Sieghart, W., Mayer, A., Drexler, G., 1983. Properties of [3H]flunitrazepam binding to different benzodiazepine binding proteins. Eur J Pharmacol 88, 291–299. https://doi.org/10.1016/0014-2999(83)90579-4

Waszkielewicz, A.M., Cegła, M., Żesławska, E., Nitek, W., Słoczyńska, K., Marona, H., 2015. N-[(2,6-Dimethylphenoxy)alkyl]aminoalkanols-their physicochemical and anticonvulsant properties. Bioorg Med Chem 23, 4197–4217. https://doi.org/10.1016/j.bmc.2015.06.045

Wilcox KS, Dixon-Salazar T, Sills GJ, Ben-Menachem E, White HS, Porter RJ,Dichter MA, Moshé SL, Noebels JL, Privitera MD, et al. (2013) Issues related to development of new antiseizure treatments. Epilepsia 54 (Suppl 4):24–34.

Witkin, J.M., Cerne, R., Wakulchik, M., S, J., Gleason, S.D., Jones, T.M., Li, G., Arnold, L.A., Li, J.-X., Schkeryantz, J.M., Methuku, K.R., Cook, J.M., Poe, M.M., 2017. Further evaluation of the potential anxiolytic activity of imidazo[1,5-a][1,4]diazepin agents selective for α2/3-containing GABAA receptors. Pharmacol Biochem Behav 157, 35–40. https://doi.org/10.1016/j.pbb.2017.04.009

Witkin, J.M., Li, G., Golani, L.K., Xiong, W., Smith, J.L., Ping, X., Rashid, F., Jahan, R., Cerne, R., Cook, J.M., Jin, X., 2020. The Positive Allosteric Modulator of α2/3-Containing GABAA Receptors, KRM-II-81, Is Active in Pharmaco-Resistant Models of Epilepsy and Reduces Hyperexcitability after Traumatic Brain Injury. J. Pharmacol. Exp. Ther. 372, 83–94. https://doi.org/10.1124/jpet.119.260968

Witkin, J.M., Lippa, A., Smith, J.L., Jin, X., Ping, X., Biggerstaff, A., Kivell, B.M., Knutson, D.E., Sharmin, D., Pandey, K.P., Mian, M.Y., Cook, J.M., Cerne, R., 2022. The imidazodiazepine, KRM-II-81: An example of a newly emerging

generation of GABAkines for neurological and psychiatric disorders. Pharmacol Biochem Behav 173321. https://doi.org/10.1016/j.pbb.2021.173321

Witkin, J.M., Smith, J.L., Ping, X., Gleason, S.D., Poe, M.M., Li, G., Jin, X., Hobbs, J., Schkeryantz, J.M., McDermott, J.S., Alatorre, A.I., Siemian, J.N., Cramer, J.W., Airey, D.C., Methuku, K.R., Tiruveedhula, V.V.N.P.B., Jones, T.M., Crawford, J., Krambis, M.J., Fisher, J.L., Cook, J.M., Cerne, R., 2018. Bioisosteres of ethyl 8-ethynyl-6-(pyridin-2-yl)-4H-benzo[f]imidazo [1,5-a][1,4]diazepine-3-carboxylate (HZ-166) as novel alpha 2,3 selective potentiators of GABAA receptors: Improved bioavailability enhances anticonvulsant efficacy. Neuropharmacology 137, 332–343. https://doi.org/10.1016/j.neuropharm.2018.05.006

Woodbury, L.A., Davenport, V.D., 1952. Design and use of a new electroshock seizure apparatus, and analysis of factors altering seizure threshold and pattern. Arch Int Pharmacodyn Ther 92, 97–107.

Zangrandi, L., Schwarzer, C., 2022. The Kappa Opioid Receptor System in Temporal Lobe Epilepsy. Handb Exp Pharmacol 271, 379–400. https://doi.org/10.1007/164_2021_444

Zhang, D., Wei, C., Hop, C., Wright, M. R., Hu, M., Lai, Y., Khojasteh, S. C., & Humphreys, W. G. (2021). Intestinal Excretion, Intestinal Recirculation, and Renal Tubule Reabsorption Are Underappreciated Mechanisms That Drive the Distribution and Pharmacokinetic Behavior of Small Molecule Drugs. *Journal of medicinal chemistry*, *64*(11), 7045–7059. https://doi.org/10.1021/acs.jmedchem.0c01720.

JPET Fast Forward. Published on February 6, 2023 as DOI: 10.1124/jpet.122.001362
This article has not been copyedited and formatted. The final version may differ from this version.

JPET Fast Forward. Published on February 6, 2023 as DOI: 10.1124/jpet.122.001362
This article has not been copyedited and formatted. The final version may differ from this version.

Tables.

Table 1. Primary and secondary binding data for the three compounds studied.

Compound	Receptor	Primary (mean % inhibition)	Secondary (K_i in nM)	Fold Selectivity
FR-II-60	BZP	99.1	34.0	NA
	5-HT_{1A}	26.7	NA	NA
	KOR	53.4	1847	54.3
	PBR	40.1	NA	NA
	Sigma2	60.5	4396	129
KPP-III-34	BZP	92.2	49.6	NA
	5-HT_{1A}	50.2	2027	40.9
	KOR	90.6	282	5.7
	PBR	63.9	662	13.3
KPP-III-51	BZP	92.0	182	NA
	5-HT_{1A}	51.5	2108	11.6
	KOR	65.6	1292	7.10
	PBR	74.3	1263	6.94

Secondary binding were determined only for primary binding sites for which > 50% inhibition was achieved. Only these sites are reported in the table. The secondary binding data are the mean of two determinations.

BZP: Benzodiazepine binding site assessed by inhibition of [^{3}H]-flunitrazepam binding in rat brain homogenates

5-HT_{1A}: Serotonin 1A receptor was assessed by inhibition of [^{3}H]-WAY100635 binding

KOR: Kappa opioid receptor was assessed by inhibition of [^{3}H]-U69593 binding

PBR: Peripheral benzodiazepine receptor sites were assessed by inhibition of [^{3}H]-PK11195 in rat brain homogenates

NA: not applicable

Table 2. Effects of the test compounds given i.p. in two acute seizure provocation models and on rotarod performance of male, CF1 mice[1].

FR-II-60

Assay	Dose (mg/kg, IP)	Number Affected/ Number Tested @ 0.5 h	Number Affected/ Number Tested @ 2 h
6 Hz	30	3/4*	1/4
	100	3/4*	3/4*
	300	3/4*	4/4*
MES	30	2/4	1/4
	100	4/4*	4/4*

	300	4/4*	4/4*
Rotorod	30	4/8	0/8
	100	6/8*	5/8
	300	8/8*	7/8*

KPP-III-34

6 Hz	30	0/4	0/4
	100	3/4*	0/4
	300	3/4*	2/4
MES	30	0/4	0/4
	100	2/4	0/4*
	300	2/4	3/4*
Rotorod	30	0/8	0/8
	100	2/8	0/8
	300	8/8*	2/8

KPP-III-51

6 Hz	30	0/4	0/4
	100	0/4	0/4
	300	0/4	2/4
MES	30	0/4	0/4
	100	0/4	0/4[&]
	300	0/4	0/4
Rotorod	30	0/8	0/8
	100	2/8	0/8
	300	8/8*[#]	3/8

[1]Historical controls were employed where under vehicle conditions there was neither any protection from seizures nor impairment of rotarod performances (C, Metcalf, University of Utah, personal communication).

[*]$P < 0.05$
[&]Death associated with tonic seizure
[#]Unable to grasp rotarod.

Table 3. Maximal concentrations of compounds and AUCs in the plasma and brains of rats after oral dosing (2 mg/kg), as well as the brain-to-plasma ratios of maximal concentrations and AUCs (Kp, partition coefficient) derived from these values.

Compound	**C_{max} (Plasma)**	**C_{max} (Brain)**	**C_{max} (Brain/Plasma)**	**AUC_{0-24} (plasma)**	**AUC_{0-24} (brain)**	**Kp (partition coefficient)**
FR-II-60	22.4	391.2	17.46	24.44	402.92	16.49
KPP-III-34	228.2	259.2	1.14	462.18	1014.60	2.20
KPP-III-51	39.3	69.6	1.77	96.13	430.25	4.48

Concentrations are in nmol/L and nmol/kg, for plasma and brain, respectively. AUCs are in ng · h/ml and ng · h/g

JPET Fast Forward. Published on February 6, 2023 as DOI: 10.1124/jpet.122.001362
This article has not been copyedited and formatted. The final version may differ from this version.

Table 4. Protection against lethality induced by 75 mg/kg PTZ (s.c.) after oral administration (60 min prior) of test compounds in male, C57BL/6N mice.

Compound	**Lethality/ Number Tested**	
Vehicle	12/15	
FR-II-60 (10 mg/kg)	0/6*	
FR-II-60 (30 mg/kg)	1/6*	
KPP-III-34 (10 mg/kg)	0/6*	
KPP-III-34 (30 mg/kg)	2/6	
KPP-III-51 (10 mg/kg)	1/6*	
KPP-III-51 (30 mg/kg)	4/6	

Shown are the number of mice that died/number of mice tested.
*P < 0.05

Table 5. Time course of the anticonvulsant effects of orally administered KPP-III-34 on PTZ-induced convulsions in rats.

Dose (mg/kg)	**0.25 h**	**0.5 h**	**1 h**	**2 h**	**4 h**
5	1/4	1/4	0/4	1/4	0/4
20	3/4*	4/4*	3/4*	3/4*	2/4
50	6/8*	8/8*	6/8*	7/8*	7/8*

Male, Sprague-Dawley rats were tested for seizure induction by PTZ at different times after dosing of KPP-III-34. Data are shown as number of rats protected/number of rats tested. * $p < 0.05$ compared to vehicle control.

Table 6. Dose-response of orally administered KPP-III-34 on PTZ-induced convulsions in rats

Dose (mg/kg)	**Number Protected /Number Tested**	**Adverse Events**
5	1/4	0/8
10	1/8	0/8
20	5/8	0/8
50	8/8*	0/8

Male, Sprague-Dawley rats were tested at 0.5 h post dosing of KPP-III-34
Data are shown as the number of rats protected/number of rats tested
* $p < 0.05$ compared to vehicle control

Table 7. Effects of KPP-III-34 on orally administered KPP-III-34 on corneal kindling in male, CF1 mice.

Dose (mg/kg)	Number Protected /Number Tested	Individual Seizure Scores	Mean Seizure Score (S.E.M)
3.5	1/8	0,4,5,4,4,5,5,4	3.88 (0.58)
15	6/8*	0,0,0,4,0,5,0,0	1.12 (0.74)**
30	5/8	0,0,3,0,4,4,0,0	1.38 (0.68)*
60	6/8*	0,0,0,0,0,2,0,3	0.62 (0.42)***
120	8/8*	0,0,0,0,0,0,0,0	0.00 (0.00)***

KPP-III-34 was given orally, 1 h prior to corneal stimulation and given a seizure severity score from 0 to 5 as described in Methods.
A mouse was considered protected from seizures when they did not exhibit any seizure signs (Methods); such mice were given a score of 0 for their seizure score.
*P < 0.05; **P < 0.01; ***P < 0.001 compared to effects at 3.5 mg/kg

Table 8. Docking scores of alprazolam, FR-II-60, and KPP-III-34, and KPP-III-51.

Compound	Docking score (Binding affinity in kcal/mol)
alprazolam	-10.8
FR-II-60	-9.5
KPP-III-34	-9.1
KPP-III-51	-9.6

Data on KPP-III-51 are from Pandey et al. (2020)

Table 9. Comparative Effects of KPP-III-34 and KRM-II-81*

Assay	KPP-III-34	KRM-II-81	KRM-II-81 Reference
C_{max} Plasma - rat	228 nM	395 -1832 nM	Golani et al., 2022a; Mian et al., 2022
C_{max} Brain - rat	259 nM	594 - 678 nM	Golani et al., 2022a;

JPET Fast Forward. Published on February 6, 2023 as DOI: 10.1124/jpet.122.001362
This article has not been copyedited and formatted. The final version may differ from this version.

			Mian et al., 2022
C_{max} – Brain/Plasma	1.14	0.32 – 1.7	Golani et al., 2022a; Mian et al., 2022
AUC_{0-24} Plasma – rat	1064 nM	2161 - 3589 nM	Golani et al., 2022a; Mian et al., 2022
AUC_{0-24} Brain - rat	2336 nM	2343 – 2690 nM	Golani et al., 2022a; Mian et al., 2022d
PTZ clonus - mouse	30 mg/kg	10 mg/kg	Golani et al., 2021; Mian et al., 2022
PTZ tonus - mouse	30 mg/kg	10 mg/kg	Golani et al., 2022a; Mian et al., 2022
PTZ lethality - mouse	10 mg/kg	10 mg/kg	Golani et al., 2022a; Mian et al., 2022
6 Hz (44 mA) – mouse	200 mg/kg	50 mg/kg	Witkin et al., 2018
Corneal kindling - mouse	13 mg/kg	8 mg/kg	Witkin et al., 2020
Mesial temporal lobe seizures – mouse	30 mg/kg	15 mg/kg	Witkin et al., 2020
Rotarod – mouse	120 mg/kg	100 mg/kg	Ping et al., unpublished
Molecular modeling docking score	-9.1 kcal/mol	-9.4 kcal/mol	Witkin et al., 2020
Adverse events – rat	> 500 mg/kg	> 300 mg/kg	Witkin et al., 2020
Cytotoxicity	> 300 mM	> 100 mM	Poe et al., 2016
hERG binding	> 10 mM	> 100 mM	Poe et al., 2016 suppl.
BZP binding	47.4	294-554	From NIMH PDSP
5-HT1A binding	1835	29.5% inhibition	From NIMH PDSP
KOR binding	380	45.9% inhibition	From NIMH PDSP
PBR	591	435-723	From NIMH PDSP

*Data for KPP-III-34 are from the present study. In vivo data are with oral dosing.
Anticonvulsant data are minimum effective doses.
For the mesial temporal lobe seizure assay, only one dose was tested.
For the cytotoxicity assay, only 100 mM was tested for KRM-II-81.
Binding data are shown for the receptors identified in a primary screen for KPP-III-34 where >50% inhibition was observed at 10 mM. Data are expressed as K_i in nM or as % inhibition in the primary screen.

Figure Legends

Figure 1. Structures of KRM-II-81 and the structural analogs reported in this manuscript.

Figure 2. Pharmacokinetic profiles and calculated parameters of FR-II-60 in plasma and brain after oral gavage in adult male, Sprague Dawley rats (n = 3 per time point) at dose of 2 mg/kg. C_{max} – maximum concentration; t_{max} – time of maximum concentration; $AUC_{0–24}$ – area under the concentration versus time curve from zero to last measurable time point; $t_{1/2}$ - terminal elimination half-life.

Figure 3. Pharmacokinetic profiles and calculated parameters of KPP-III-34 in plasma and brain after oral gavage in adult male, Sprague Dawley rats (n = 3 per time point) at dose of 2 mg/kg. C_{max} – maximum concentration; t_{max} – time of maximum concentration; $AUC_{0–24}$ – area under the concentration versus time curve from zero to last measurable time point; $t_{1/2}$ - terminal elimination half-life.

Figure 4. Pharmacokinetic profiles and calculated parameters of KPP-III-51 in plasma and brain after oral gavage in adult male, Sprague Dawley rats (n = 3 per time point) at dose of 2 mg/kg. C_{max} – maximum concentration; t_{max} – time of maximum concentration; $AUC_{0–24}$ – area under the concentration versus time curve from zero to last measurable time point; $t_{1/2}$ - terminal elimination half-life.

Figure 5. Effects of orally administered FR-II-60, KPP-III-34, or KPP-III-51 on the latency to produce clonic (left panels) or tonic (right panels) seizures after 75 mg/kg PTZ, s.c. in male, C57BL/6N mice. *, **, *** P <0.05, 0.01, and 0.001 compared to respective vehicle control value. N=6-9 mice per group.

Figure 6. Effects of KPP-III-34 in male, C57/Bl6 mice that were created to exhibit spontaneous recurrent hippocampal discharges. N=8 mice/group.

Figure 7. Effect of orally administered diazepam (5 mg/kg), FR-II-60, and KPP-III-34 on sensorimotor coordination in female, Swiss Webster mice as assessed by rotarod performance. Data are means ± SEM (N = 10/group). ∗ ($p<0.05$) or ∗∗∗ ($p <0.001$) compared to vehicle-treated mice at the same time point.

Figure 8. A: Showing best pose of compound FR-II-60 (goldenrod) docked in 6HUO. **B**: Showing best pose of compound FR-II-60 (goldenrod) docked in 6HUO, overlay with bound alprazolam (grey) in 6HUO. α1 (aquamarine) and γ2 (orchid) subunits of α1β3γ2L $GABA_A$ receptor 6HUO. Dashed lines indicate π–π, hydrogen bond and halogen bond interactions.

Figure 9. A: Showing best pose of compound KPP-III-34 (purple) docked in 6HUO. **B**: Showing best pose of compound KPP-III-34 (purple) docked in 6HUO, overlay with bound alprazolam (grey) in 6HUO. α1 (aquamarine) and γ2 (orchid) subunits of α1β3γ2L

JPET Fast Forward. Published on February 6, 2023 as DOI: 10.1124/jpet.122.001362
This article has not been copyedited and formatted. The final version may differ from this version.

$GABA_A$ receptor 6HUO. Dashed lines indicate π–π, hydrogen bond and halogen bond interactions.

JPET Fast Forward. Published on February 6, 2023 as DOI: 10.1124/jpet.122.001362
This article has not been copyedited and formatted. The final version may differ from this version.

Fig. 1

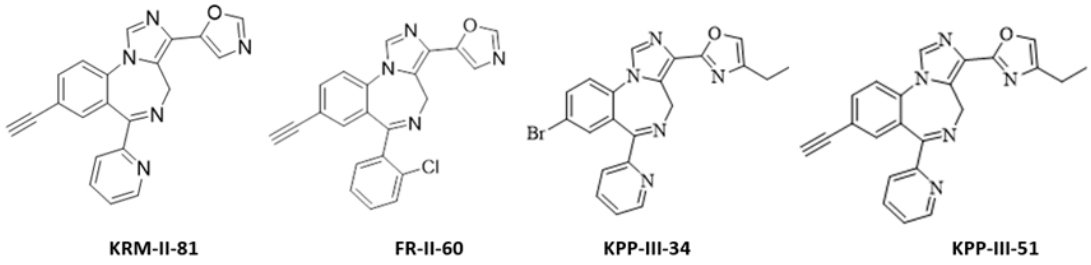

JPET Fast Forward. Published on February 6, 2023 as DOI: 10.1124/jpet.122.001362
This article has not been copyedited and formatted. The final version may differ from this version.

Fig. 2

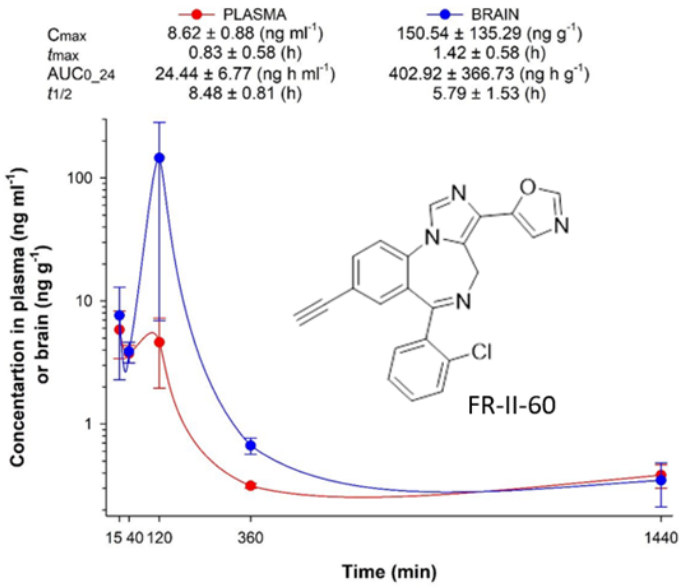

JPET Fast Forward. Published on February 6, 2023 as DOI: 10.1124/jpet.122.001362
This article has not been copyedited and formatted. The final version may differ from this version.

Fig. 3

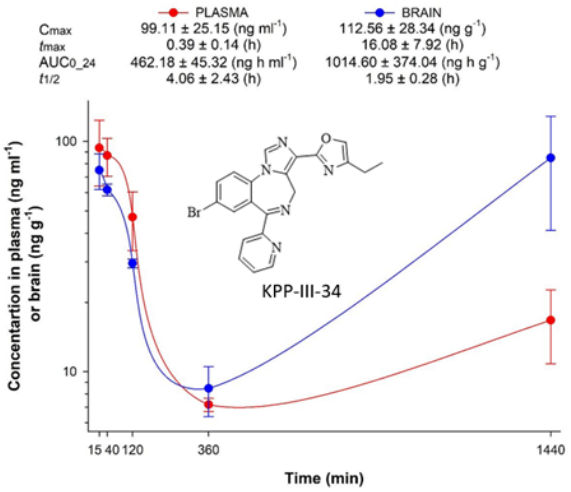

JPET Fast Forward. Published on February 6, 2023 as DOI: 10.1124/jpet.122.001362
This article has not been copyedited and formatted. The final version may differ from this version.

Fig. 4

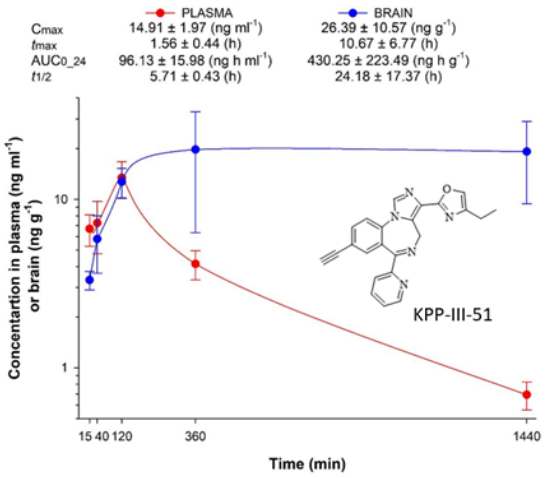

JPET Fast Forward. Published on February 6, 2023 as DOI: 10.1124/jpet.122.001362
This article has not been copyedited and formatted. The final version may differ from this version.

Fig. 5

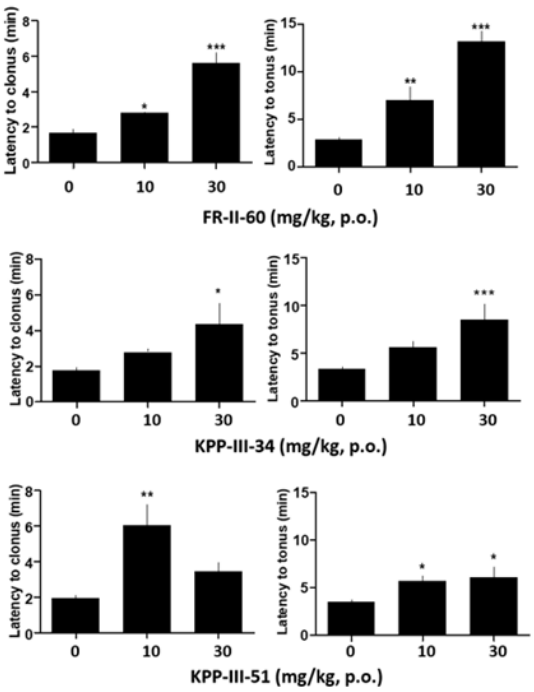

JPET Fast Forward. Published on February 6, 2023 as DOI: 10.1124/jpet.122.001362
This article has not been copyedited and formatted. The final version may differ from this version.

Fig. 6

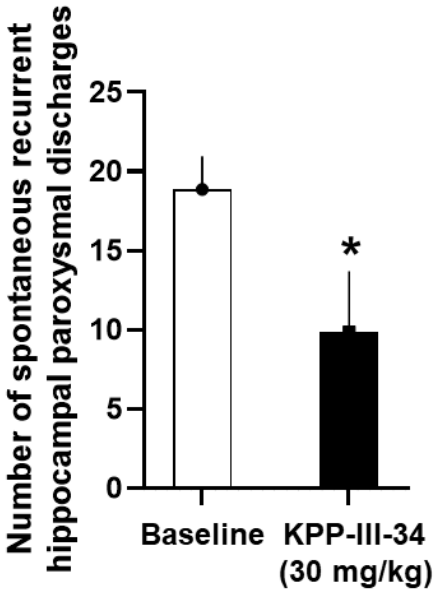

JPET Fast Forward. Published on February 6, 2023 as DOI: 10.1124/jpet.122.001362
This article has not been copyedited and formatted. The final version may differ from this version.

Fig. 7

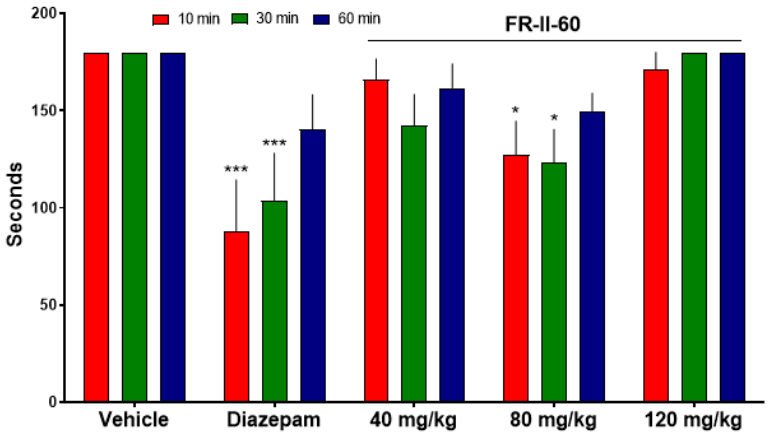

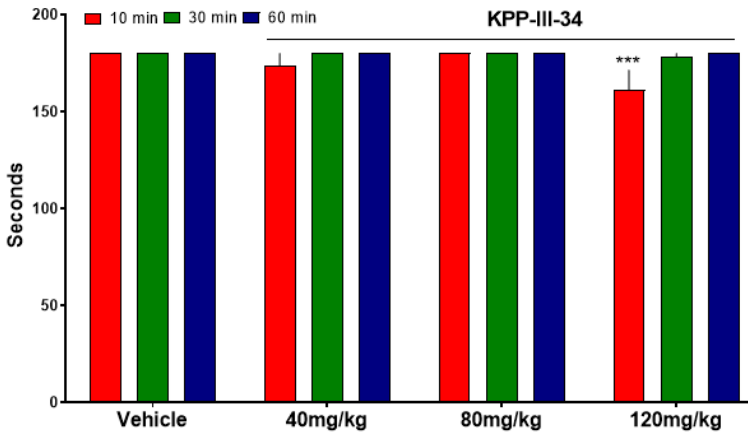

JPET Fast Forward. Published on February 6, 2023 as DOI: 10.1124/jpet.122.001362
This article has not been copyedited and formatted. The final version may differ from this version.

Fig. 8

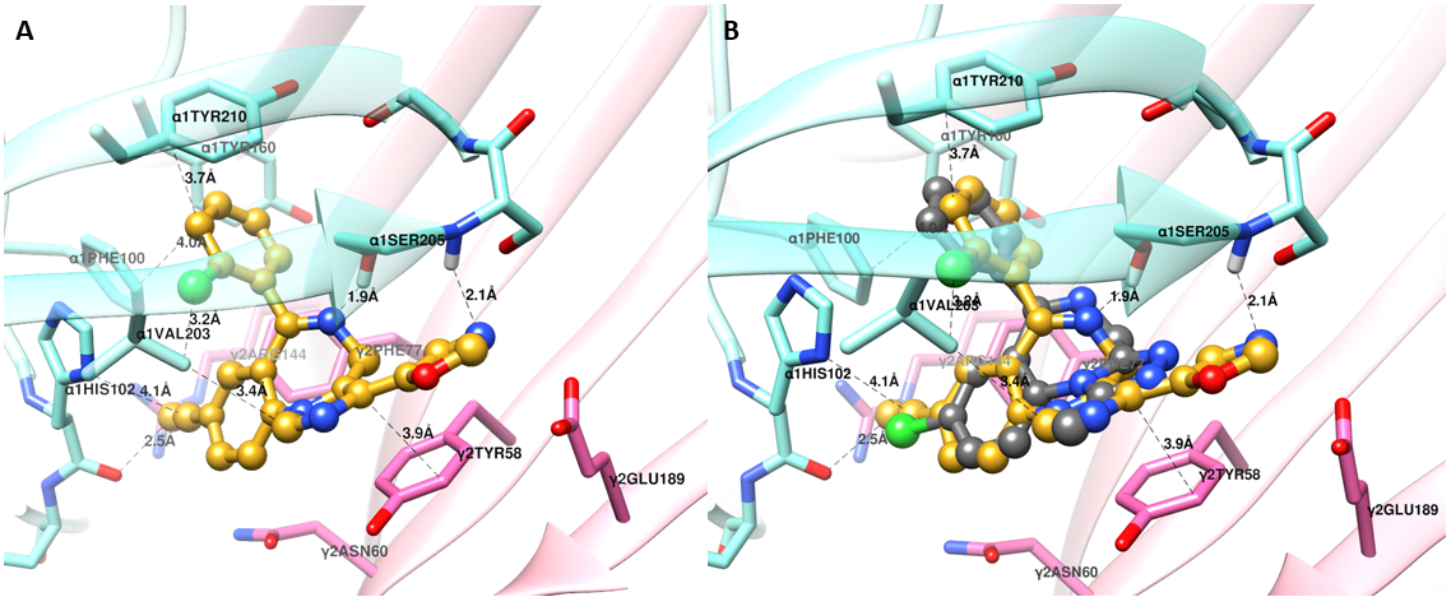

JPET Fast Forward. Published on February 6, 2023 as DOI: 10.1124/jpet.122.001362
This article has not been copyedited and formatted. The final version may differ from this version.

Fig. 9